ACS OMEGA

Open Access

http://pubs.acs.org/journal/acsodf

Article

Synthesis of Carboxylate-Dialdehyde Cellulose to Use as a Component in Composite Thin Films for an Antibacterial Material in Wound Dressing

Tanpong Chaiwarit,* Kwanjit Duangsonk, Sastra Yuantrakul, Baramee Chanabodeechalermrung, Waristha Khangtragool, Claire-Hélène Brachais, Odile Chambin, and Pensak Jantrawut

Cite This: *ACS Omega* 2024, 9, 44825−44836

Read Online

ACCESS | Metrics & More | Article Recommendations

ABSTRACT: Wound infections can lead to life-threatening infection and death. Antibacterial materials from biopolymers in the form of films are a promising strategy for wound dressings. Carboxylate-dialdehyde cellulose (CDAC) is a proper candidate for use as an antibacterial material due to its biocompatibility, nontoxicity, and antibacterial property. Additionally, CDAC can be synthesized from cellulose through environmentally friendly and nontoxic methods. Thus, this study aims to synthesize CDAC from microcrystalline cellulose (MCC) PH102 and use it in composite films for an antibacterial application. The CDAC was synthesized using Fe^{2+}/H_2O_2, followed by $NaIO_4$ oxidation. The obtained CDAC was characterized in terms of carboxylate and aldehyde content as well as FTIR and XRD spectra. The CDAC was mixed with HPMC in different ratios to prepare films. To determine the optimal formulation for clindamycin HCl loading, the films were evaluated for morphology, mechanical properties, and swelling ratio. Finally, the films containing clindamycin HCl were evaluated for drug loading content, *in vitro* drug release, and antibacterial activity. This study found that CDAC contained 2.1 ± 0.2 carboxylate and 4.15 ± 0.2 mmol/g of aldehyde content. The FTIR spectra confirmed the successful synthesis. X-ray diffractograms indicated that CDAC was less crystalline than MCC. The film, consisting of CDAC and HPMC E50 in the ratio of 2:1 (D2H1), was identified as the most suitable for clindamycin HCl loading due to its superior appearance, mechanical strength, and swelling properties compared to other formulations. D2H1 exhibited a high drug loading capacity (91.49 ± 5.48%) and demonstrated faster drug release than the film composed only of HPMC because of the higher swelling ratio and lower mechanical strength. This formulation was effective against *Staphylococcus aureus* (MSSA), *S. aureus* (MRSA), and *Pseudomonas aeruginosa*. Furthermore, the D2H1 film containing clindamycin HCl showed a larger inhibition zone against these bacteria, likely due to a synergistic effect. This study found that CDAC has the potential to be applied as an antibacterial material for wound dressing.

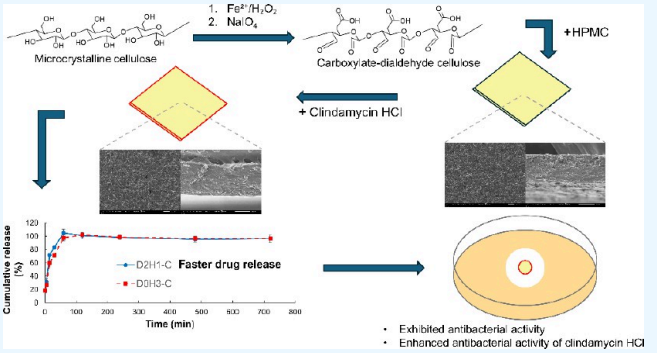

INTRODUCTION

The skin is the body's largest and most significant organ, serving as a protective barrier against direct environmental exposure and foreign substances.[1,2] Physical, thermal, chemical, and radiogenic damage can cause defects or breaches in the skin, leading to wound formation.[3] Inadequate wound dressing not only hinders the healing process but also can result in bacterial infections, potentially causing life-threatening conditions, such as sepsis and death. In addition, bacterial resistance to antibiotics is a significant challenge in the treatment of infected wounds. Therefore, it is interesting and important to develop antibacterial material for wound dressing, which enhances antibacterial activity for drug-resistant bacteria. There are various methods to promote wound healing, with wound dressings being the most popular due to their noninvasive nature. Wound dressings are in different forms including film, hydrogels, hydrocolloids, foams, and hydrofibers.[4] Among these, film dressings are widely known as one of the favored options. There are various advantages of film dressings, including providing ease of application, reducing pain, protecting the wound from external contaminants, and allowing inspection of the wound bed without the need to remove the dressing.[4,5]

Received: September 9, 2024
Revised: October 9, 2024
Accepted: October 15, 2024
Published: October 24, 2024

For decades, the applications of biopolymers have gained widespread interest in both medical and pharmaceutical fields due to their natural abundance, low-cost production, biocompatibility, and nontoxicity.[6] There are various types of biopolymers, for instance, cellulose, chitosan, gelatin, and collagen.[1] Among these, cellulose, a linear polysaccharide composed of glucose units cross-linked with β-1,4-glycosidic bonds, is the most plentiful resource. Furthermore, cellulose's ease of modification makes it an excellent starting material for novel biological applications.[1,7,8] The hydroxyl groups on the surface of cellulose are frequently subjected to a variety of chemical treatments, for example, carboxymethylation, methylation, hydroxyethylation, 2,2,6,6-tetramethylpiperidine 1-oxyl (TEMPO) oxidation, and peroxidation.[8] Carboxylated cellulose, produced through carboxylation, exhibits improved dispersibility and hydrophilicity due to the presence of negatively charged carboxyl groups.[2] Although several methods exist to prepare carboxylated cellulose, some present drawbacks. For example, TEMPO oxidation employs a toxic reagent that poses risks to both the environment and living organisms. Ammonium persulfate (APS) oxidation, regardless of its low toxicity, demands a large consumption and a high expense of chemicals. To overcome these challenges, a novel reaction process utilizing a nontoxic and environmentally friendly Fe^{2+}/H_2O_2 solution has been developed, producing carboxylated cellulose with high carboxyl content.[9] 2,3-Dialdehyde cellulose, a cellulose derivative, can be prepared by a periodate reaction. Using periodate ions (IO_4^-) as an oxidizing agent, the ions selectively cleave the C_2-C_3 bonds of the glucopyranoside ring, resulting in converting hydroxyl groups to two aldehydes per unit.[8,10] Notably, 2,3-dialdehyde cellulose exhibits good film-forming properties.[11] Furthermore, it possesses many desirable characteristics to be utilized in wound dressing such as low toxicity, biodegradation, compatibility, and antimicrobial activities against *Staphylococcus aureus* and *Escherichia coli*.[1] Some studies have prepared composite films of dialdehyde cellulose with other polymers through cross-linking. However, it is crucial to retain the inherent antibacterial properties of dialdehyde cellulose for the treatment of infected wounds. A film composed of dialdehyde cellulose and HPMC could preserve the free aldehyde groups within the dialdehyde cellulose molecules, thereby maintaining its antibacterial activity, as HPMC does not cross-link with the aldehyde groups of dialdehyde cellulose. Although methods for introducing carboxylate and dialdehyde groups into cellulose have been explored, and some studies have combined dialdehyde cellulose with polymers such as chitosan and poly(vinyl alcohol), research on film formulations comprising carboxylate-dialdehyde cellulose and HPMC remains limited. Clindamycin is a semisynthetic antibiotic derived from lincomycin and an effective antibiotic for treating serious skin and soft tissue infections caused by *S. aureus*, such as burn wound infections.[12−14]

This study aimed to develop a composite thin film for wound dressings based on carboxylate-dialdehyde cellulose (CDAC) with its own antibacterial activity and synergies of this property by loading clindamycin. The CDAC was synthesized using single-step Fe_{2+}/H_2O_2, followed by sodium periodate ($NaIO_4$) oxidation (Figure 1). The CDAC was formulated into CDAC composite films with different ratios of CDAC and HPMC E50 and loaded with clindamycin. The films were characterized to identify the optimal formulation through assessments of morphology, mechanical properties, swelling ratio, drug content, *in vitro* drug release, and antibacterial activity.

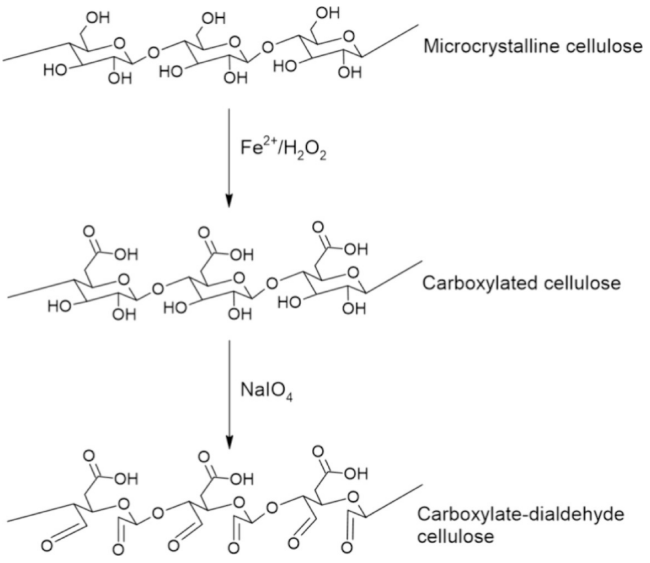

Figure 1. Reaction scheme of the carboxylate-dialdehyde cellulose synthesis.

MATERIALS

Microcrystalline cellulose (MCC) PH102 (conformed with NF, Ph. Eur., and JP, 100 μm, 211 degrees of polymerization) was purchased from Dupont (Delaware, USA). Iron(II) sulfate 7-hydrate ($FeSO_4{\cdot}7H_2O$), sodium metaperiodate ($NaIO_4$), and potassium chloride (KCl) were purchased from Kemaus (New South Wales, Australia). Hydrogen peroxide (H_2O_2) was purchased from QArc (Auckland, New Zealand). Sodium chloride (NaCl), disodium hydrogen phosphate (Na_2HPO_4), and potassium dihydrogen orthophosphate (KH_2PO_4) were purchased from RCI Laboratories (Bangkok, Thailand). Hydroxypropyl methylcellulose (HPMC) E50 was purchased from LOTTE Fine Chemical (Seoul, Korea).

EXPERIMENTAL SECTION

Synthesis of Carboxylated Cellulose. The method for synthesizing carboxylated cellulose was adapted from a previous study.[9] One gram of MCC was mixed with 50 mL of the solution containing different weights of $FeSO_4{\cdot}7H_2O$ 0.0037−0.0146 g (equivalent to $FeSO_4$ 0.002−0.008 g) and 30 mL of H_2O_2 in an ultrasonic bath for 10 min, followed by heating at 60 or 80 °C for 4−6 h. Afterward, the mixture was centrifuged at 8000 rpm for 20 min to collect the carboxylated cellulose and remove the supernatant. The carboxylated cellulose was washed several times with deionized water by centrifugation at 8000 rpm for 20 min until the pH of the supernatant was equal to that of the deionized water. The carboxylated cellulose was dried using a freeze-dryer (Christ Beta 2-8 LD Plus, Osterode am Harz, Germany).

Determination of Carboxyl Content. The method for determining the carboxyl content of carboxylated cellulose was adapted from a previous study.[14] Carboxyl content was determined by using conductometric titration. Twenty milligrams of carboxylated cellulose was homogeneously dispersed in 60 mL of 0.01 M NaOH in an ultrasonic bath for 20 min. Then, the suspension was stirred for 24 h. The pH of the suspension was adjusted to 3 by adding 0.01 M HCl. The

https://doi.org/10.1021/acsomega.4c08298
ACS Omega 2024, 9, 44825−44836

suspension was titrated with 0.01 M NaOH until the pH increased to 10 at a rate of 0.1 mL/min. The carboxyl content was calculated using eq 1.

$$\text{carboxyl content (mmol/g)} = \frac{C_{\text{NaOH}}(V_2 - V_1)}{W} \quad (1)$$

where C_{NaOH} is the concentration of NaOH (M), $V_2 - V_1$ is the volume of NaOH (mL) in the plateau, and W is the weight of carboxylated cellulose (g).

Synthesis of CDAC. The method for synthesizing CDAC was adapted from previous studies.[8,15] A 10 g portion of carboxylated cellulose was added to 500 mL of deionized water containing 10 g of NaOH and 10 g of $NaIO_4$. The mixture was stirred at 25 °C for 19 h in a dark place. At the end of the reaction, ethanol was added to quench the residual periodate. The mixture was centrifuged at 8000 rpm for 20 min to precipitate the CDAC. The CDAC was washed several times with deionized water by centrifugation at 8000 rpm to remove any remaining $NaIO_4$, until the pH was neutral. Finally, CDAC was dried using a freeze-dryer. The yield (%) of carboxylated cellulose and CDAC was calculated using eqs 2 and 3, respectively.

$$\text{yield of carboxylated cellulose (\%)} = \frac{\text{weight of carboxylated cellulose (g)}}{\text{weight of MCC (g)}} \times 100 \quad (2)$$

$$\text{yield of CDAC (\%)} = \frac{\text{weight of CDAC (g)}}{\frac{\text{weight of MCC (g)}}{\text{weight of carboxylated cellulose (g)}}} \times 100 \quad (3)$$

Determination of Aldehyde Content. The method for determining aldehyde content was described in a previous study.[10] Briefly, 0.5 g of CDAC was homogeneously dispersed in 25 mL of deionized water. Then, 20 mL of 0.05 g/mL hydroxylamine HCl, adjusted to pH 5 using NaOH, was added to the dispersion. The mixture was stirred for 4 h at 40 °C, followed by titration with 0.1 M NaOH. The end point was determined when the pH reached 5. Each experiment was conducted in triplicate. The aldehyde content was calculated using eqs 4 and 5.

$$\text{aldehyde content (mmol/g)} = \frac{(V_1 - V_2) \times C_{\text{NaOH}}}{m} \quad (4)$$

$$\text{aldehyde content (\%)} = \frac{C_{\text{NaOH}}(V_1 - V_2) \times 162}{m \times 1000} \times 100 \quad (5)$$

where C_{NaOH} is the concentration of NaOH (M), V_1 is the consumption of 0.1 NaOH in a titration of CDAC (mL), V_2 is the volume of 0.1 NaOH (mL), which was used to titrate the same weight of MCC, and m is the mass of CDAC (g).

Fourier Transform Infrared (FTIR) Spectrophotometer. The FTIR analysis was performed using a Fourier transform infrared spectrophotometer FT/IR-4700 (Jasco, Tokyo, Japan) at a resolution of 4 cm^{-1} in transmittance mode. The samples were measured in the range 500−4000 cm^{-1}.

X-ray Diffractometry (XRD). The crystalline states of CDAC, carboxylated cellulose, and MCC were analyzed using an analytical X-ray diffractometer (MiniFlex ll, Rigaku Corporation, Tokyo, Japan) under the following conditions: 40 kV voltage, 0.4 s/step counting rate, and a scanning range from 5 to 70°. The crystallinity index (CrI) was calculated using eq 6.[16]

$$\text{CrI (\%)} = \frac{I_{200} - I_{\text{am}}}{I_{200}} \times 100 \quad (6)$$

where I_{200} is the maximum intensity of the (200) diffraction at the 2θ value of about 22.2° and I_{am} is the intensity diffraction at a 2θ value of around 18°.

Preparation of CDAC Composite Films. The film formulations consisted of different ratios of CDAC and HPMC E50 (Table 1). CDAC was homogeneously dispersed in 95.8 g of deionized water at 80 °C for 4 h, after which HPMC E50 was added. Glycerol (1.2 g) was added as a plasticizer, and the mixture was stirred at room temperature for 1 h. The mixture (15 g) was poured into a Petri dish (9 mm in diameter), followed by drying in a hot air oven at 40 °C for 18 h. To prepare the CDAC composite film loading drug, clindamycin HCl (1.1 g, equivalent to 1 g of clindamycin base) was dissolved in the polymeric solution before pouring it into a Petri dish.

Table 1. Formulations of CDAC Composite Films

	composition			
formulations	CDAC (g)	HPMC (g)	DI water (g)	glycerol (g)
D3H0	3	0	95.8	1.2
D2H1	2	1	95.8	1.2
D1.5H1.5	1.5	1.5	95.8	1.2
D1H2	1	2	95.8	1.2
D0H3	0	3	95.8	1.2

Morphological Examination. The appearance of the films was assessed by visual inspection, and the thickness of the films was measured with a micrometer (3203-25A, INSIZE Co., Ltd., Suzhou, China). All film formulations were cut and fixed to an aluminum stub with adhesive carbon tape, followed by gold coating for 1 min. The surface and cross-sectional characteristics were observed at 100× and 500× magnifications, respectively, using a scanning electron microscope (SEM) (JEOL JCM-7000 NeoScope Benchtop, Tokyo, Japan) at 15 kV in low vacuum mode.

Mechanical Properties Test. The mechanical properties of the films were investigated using a TX.TAplus texture analyzer (Stable Micro Systems, Surrey, UK) with a load cell of 5 kg (0.001 N of sensitivity) in compression mode. The analytical probe was a plane flat-faced cylindrical stainless-steel surface (2 mm in diameter). The sample was fixed to the heavy-duty platform, and the test speed was 2.00 mm/s. Each experiment was performed six times at room temperature. The mechanical properties, for instance, puncture strength and Young's modulus, were calculated using eqs 7 and 8, respectively.[17]

$$\text{puncture strength} = \frac{F_{\text{max}}}{A} \quad (7)$$

where F_{max} is the force at the film break point (N) and A is the film surface area in contact with the probe surface (mm^2).

$$\text{Young's modulus} = \frac{\text{slope}}{\text{film thickness} \times \text{probe speed}} \quad (8)$$

https://doi.org/10.1021/acsomega.4c08298
ACS Omega 2024, 9, 44825−44836

Table 2. Carboxyl Content and Yield of Carboxylated Cellulose from Various Conditions[a]

number	conditions			carboxyl content (mmol/g)	yield (%)
	$FeSO_4 \cdot 7H_2O$ (g)	time (h)	temperature (°C)		
1	0.0037	4	60	0.6 ± 0.1a	92.6 ± 2.7a
2	0.0037	4	80	0.8 ± 0.1a	91.5 ± 3.9a
3	0.0037	6	60	1.4 ± 0.2b,d	88.7 ± 4.5a,b
4	0.0037	6	80	1.5 ± 0.2b,d	86.1 ± 3.2a,b
5	0.0073	4	60	1.3 ± 0.2b	88.5 ± 4.1a,b
6	0.0073	4	80	1.5 ± 0.1b,d	89.4 ± 2.9a
7	0.0073	6	60	2.1 ± 0.2c	82.4 ± 3.1b,c
8	0.0073	6	80	2.2 ± 0.1c	77.8 ± 3.5c,d
9	0.0146	4	60	1.7 ± 0.1d	70.2 ± 4.2d,e
10	0.0146	4	80	1.8 ± 0.2d	67.4 ± 3.5e
11	0.0146	6	60	2.0 ± 0.1c	64.5 ± 3.9e
12	0.0146	6	80	2.0 ± 0.3c,d	62.6 ± 3.7e

[a]Values in the same column with different lowercase letters (a−e) indicate significant differences between each condition ($p < 0.05$).

where slope is obtained from the plotted graph between force (N) and time (s).

Swelling Property. CDAC composite films were cut into 2 × 2 cm^2 and weighted using an analytical balance. The films were then immersed in 10 mL of phosphate-buffered saline (PBS) pH 7.4, at 32 °C for 24 h. The films were taken from the PBS, and the excess PBS was gently absorbed using a filter paper. The films were then reweighed, and the swelling ratio was calculated using eq 9.

$$\text{swelling ratio (\%)} = \frac{W_t - W_0}{W_0} \times 100 \quad (9)$$

where W_0 is the initial weight of a sample (g) and W_t is the weight at 24 h of a sample (g).

Determination of Drug Loading Content. The CDAC composite films were cut into 2 × 2 cm^2 and stirred in 10 mL of PBS at pH 7.4 for 24 h. The sample was taken and filtered using a 0.45 μm nylon-syringe filter, and then 1 mL of sample was diluted 20 times with PBS pH 7.4 to be within the range of the standard curve. The concentration of clindamycin HCl was determined using a UV-2600i UV−visible spectrophotometer (Shimadzu, Kyoto, Japan) at 210 nm. The standard curve was prepared by dissolving clindamycin HCl in PBS pH 7.4 to obtain different concentrations of 12.5, 25, 50, 75, and 100 μg/mL. The clindamycin HCl content in the film samples was calculated using the standard curve, with a high coefficient of determination (R^2 = 0.9985) using eq 10.

$$\text{drug content (\%)} = \frac{\text{actual drug content}}{\text{theoretical drug content}} \times 100 \quad (10)$$

***In Vitro* Drug Release Profile.** The method to investigate clindamycin HCl release from films was described in a previous study.[17] The D2H1 and D3H0 films containing clindamycin HCl were cut to a square shape (2 × 2 cm^2) and immersed in PBS pH 7.4 at 32 ± 0.5 °C in a semi-static condition. At each predetermined time (1, 5, 15, 30, 60, 120, 240, 480, and 720 min.), 3 mL of media was taken and replaced in the same volume. The samples were analyzed to determine the clindamycin concentration using the UV-2600i UV−visible spectrophotometer (Shimadzu, Kyoto, Japan) at 210 nm. The data was reported in the graph plotted between cumulative release (%) and time (min).

Antibacterial Activity. The agar disk diffusion method was used to assess the antibacterial activity of the CDAC composite films. All film samples were sterilized with ethylene oxide prior to testing. The antibacterial activity test was adapted from a previous study.[18] *S. aureus* (ATCC25923) and *Pseudomonas aeruginosa* (ATCC27853) were cultured on tryptic soy agar (HiMedia, Mumbai, India) at 37 °C for 24 h, followed by incubation in tryptic soy broth (Sigma-Aldrich, St. Louis, Missouri, USA) at 37 °C under aerobic conditions for 12 h. Briefly, 100 μL of bacterial stock (OD600 = 0.1) was spread onto dried tryptic soy agar plates. The CDAC composite films (0.5 mm in diameter) were placed on the agar and incubated at 37 °C in aerobic conditions for 16−18 h. The antibacterial activity was determined by measuring the zone of inhibition using a Mitutoyo Digimatic caliper (Mitutoyo Corporation, Kanagawa, Japan). A clindamycin disk was used as a positive control.

Statistical Analysis. The significant difference between the results was investigated at a significant level of 0.05 by SPSS software (version 17; IBM Corporation, New York, USA).

RESULTS AND DISCUSSION

Carboxylated Cellulose Synthesis. The carboxyl content and yield of carboxylated cellulose obtained from the Fe^{2+}/H_2O_2 oxidation reactions are shown in Table 2. The carboxyl content tended to increase with higher concentrations of $FeSO_4$ and longer reaction times, except for the reactions at 60 and 80 °C, which showed no significant difference in carboxyl content between these temperatures. The reaction time plays a vital role in the carboxyl content. According to a previous study, 6 h was the optimal time for providing the highest carboxyl content of carboxylated cellulose obtained from Fe^{2+}/H_2O_2 oxidation reaction.[9] However, an increase in Fe^{2+} as a catalyst, along with a prolonged reaction time, resulted in a lower yield due to decomposition. The thermal stability of carboxylated cellulose decreases with longer reaction times.[20] In addition, the amount of Fe^{2+} directly influences the hydrolysis, leading to an increase in this reaction since Fe^{2+} is able to constitute an oxidizing system with high hydrolysis efficiency.[19] The optimal condition was 0.0073 g of $FeSO_4 \cdot 7H_2O$ for 6 h at 60 °C, as shown in condition 7 in Table 2. This condition provided 2.1 ± 0.2 mmol/g of carboxyl content, which was higher than that of other conditions, while also providing a sufficient yield of 82.4 ± 3.1% based on the dry weight of MCC. The carboxylated cellulose obtained from

https://doi.org/10.1021/acsomega.4c08298
ACS Omega 2024, 9, 44825−44836

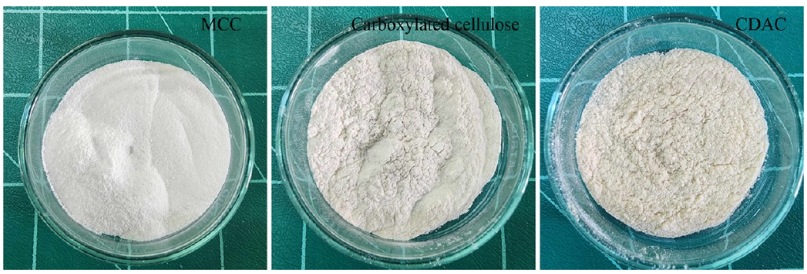

Figure 2. Photographs of MCC, carboxylated cellulose, and CDAC.

Table 3. Characteristics and Yield of Carboxylate-Dialdehyde Cellulose

sample	aldehyde content		carboxyl content (mmol/g)	yield based on carboxylate cellulose (%)	yield based on MCC weight (%)
	mmol/g	%			
carboxylate-dialdehyde cellulose (CDAC)	4.15 ± 0.2	67.23 ± 3.24	2.1 ± 0.2	76.5 ± 4.2	65.2

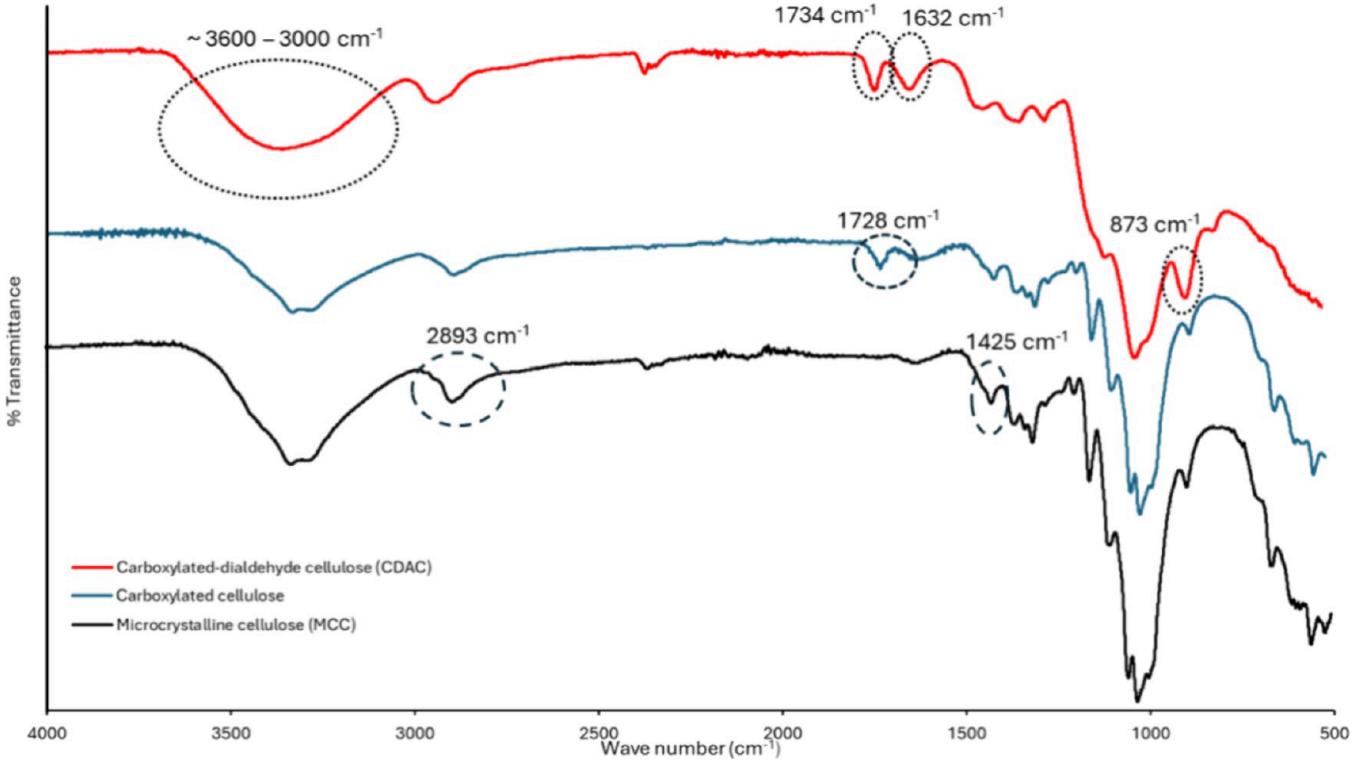

Figure 3. FTIR spectra of MCC, carboxylated cellulose, and CDAC.

this condition was white powder, whereas the MCC was a white micronized powder, as shown in Figure 2. The Fe^{2+}/H_2O_2 method for synthesizing carboxylated cellulose is practical and environmentally friendly, as it employs only $FeSO_4{\cdot}7H_2O$ and H_2O_2, both of which are readily available and nontoxic. Moreover, it is an effective method since it is able to generate a large amount of hydroxyl radicals to obtain high hydrolysis efficacy while causing low decomposition due to the high reaction rate at low temperatures.[19] At 40−80 °C, H_2O_2 is catalyzed by Fe^{2+}, generating protons (H^+) and hydroxyl radicals ($OH^{\bullet}$). H^+ protonates the β-1,4-glycosidic bonds, breaking the oxygen bridges and leading to the disintegration of the amorphous region of the cellulose. Meanwhile, OH• attacks the hydroxyl groups, producing carboxyl groups at the C-6 position, thereby forming carboxylated cellulose.[9]

CDAC Synthesis. The obtained CDAC after freeze-drying appeared as a pale-yellow powder, in contrast to the white powders of carboxylated cellulose and MCC (Figure 2). The color change might be attributed to the oxidation process involving periodate. The aldehyde content of CDAC was 4.15 ± 0.2 mmol/g, equivalent to 67.23 ± 3.24% (Table 3). The aldehyde content was higher than that in a previous study (2.84 ± 0.02 mmol/g)[22] under similar oxidant concentrations with a higher temperature. However, it was lower than the aldehyde content (6.4 ± 0.3 mmol/g) obtained in another study, which used similar synthesis conditions to produce dialdehyde cellulose.[15] This difference could be explained by the use of carboxylated cellulose as the starting material in the present study, as opposed to MCC. The yield of CDAC was 76.5 ± 4.2% based on the dry weight of carboxylated cellulose, which corresponds to 65.2% relative to the dry weight of the

https://doi.org/10.1021/acsomega.4c08298
ACS Omega 2024, 9, 44825−44836

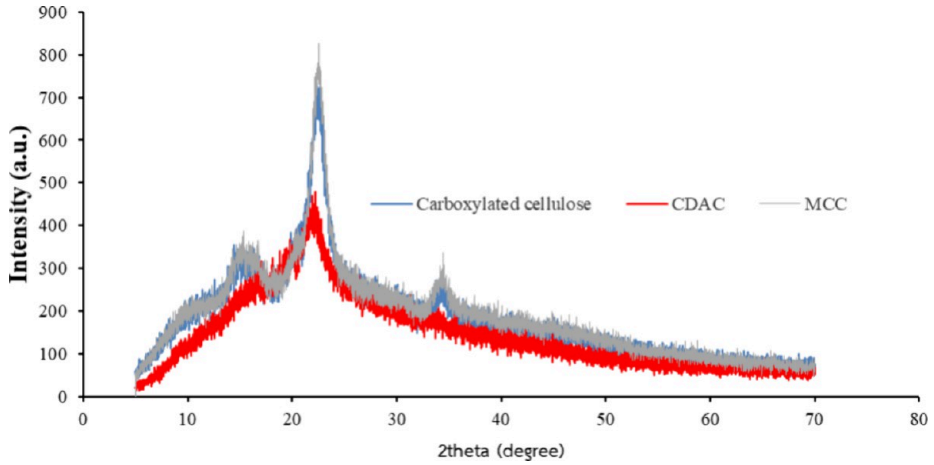

Figure 4. X-ray diffractograms of MCC, carboxylated cellulose, and CDAC.

initial MCC. The rate of cellulose oxidation to dialdehyde cellulose using $NaIO_4$ depends on the temperature, oxidant concentration, and reaction time. Beyond 50 °C, the periodate ion decomposes to iodine, which can react with cellulose to form dialdehyde groups.[21,22] Although higher temperatures can accelerate the oxidation reaction, they can also lead to the decomposition of $NaIO_4$, leading to lower aldehyde contents due to the reaction inefficiency and undesirable products.[22] At room temperature, the conversion of cellulose to dialdehyde cellulose would occur via a longer reaction time, resulting in the production of IO_3^- that is precipitated as XIO_3 when ethanol is added and is subsequently removed by washing.[22,23]

FTIR Characterization. The FTIR spectra of MCC, carboxylated cellulose, and CDAC are shown in Figure 3. The spectrum of carboxylated cellulose was similar to that of MCC. The O−H stretching was observed at a wavenumber range of 3600−3000 cm^{-1}. The peak of the C−H stretching was found at 2893 cm^{-1}. The peak at 1425 cm^{-1} represents H−C−H and O−C−H bending, corresponding to the chemical structure of cellulose.[9,24] However, the new peak at 1728 cm^{-1} in the FTIR spectrum of carboxyated cellulose indicates a carboxylic group (−COOH), confirming that the carboxylation of MCC to carboxylated cellulose was successful.[9] Interestingly, CDAC exhibited significant differences in the peaks, indicating a change in chemical structure. The O−H stretching range of 3600−3000 cm^{-1} was broader due to periodate oxidation. The visible increase in the peak at 1632 cm^{-1} was generated by the oxidized cellulose, possibly from the attribution of aldehyde hydration. The characteristic peaks of the aldehyde group (−CHO) were found at 1734 and 873 cm^{-1}.[15,22] The former peak (1734 cm^{-1}) represents C═O stretch vibration of the free aldehyde group, although it was barely detected, as most aldehyde groups were involved in masked forms, such as hemiacetals, hydrates, and hemialdals.[9,22,25] Furthermore, this peak also overlapped with the peak of the carboxylic group around 1728 cm^{-1}. The peak at 873 cm^{-1} corresponds to the vibration of semiacetal, since the aldehyde groups obtained from the synthesis reaction rarely exist in free form.[15]

XRD. The X-ray diffractograms of MCC, carboxylated cellulose, and CDAC are shown in Figure 4. The X-ray diffractogram of MCC exhibits the main reflections of cellulose at 16, 22.5, and 34.5°.[26] The diffractogram of carboxylated cellulose indicated that the crystalline structure remains after Fe^{2+}/H_2O_2 oxidation. This result aligns with a previous study,[9] which reported that the crystal structure is not eliminated since the Fe^{2+}/H_2O_2 reaction is able to digest the amorphous region of cellulose effectively. The intensity of the crystalline peak at 22.5° slightly decreased, and the CrI of carboxylated cellulose was 63.60%, which was lower than that of MCC (67.96% due to the partial removal of crystalline regions during the reaction.[9,27] Comparing MCC and carboxylated cellulose, the diffractogram of CDAC exhibits a remarkable decrease in the crystalline structure. The peaks at 16 and 34.5° disappeared, and the intensity at 22.5° decreased markedly. The CrI of CDAC was 42.59%, which significantly decreased from carboxylated cellulose. This result indicated that periodate oxidation could reduce the crystallinity while increasing amorphous regions. To clarify, the periodate oxidation reaction cleaves the glucopyranose ring, thereby damaging the ordered packing of cellulose while preserving the amorphous domains.[8,28] In addition, this transition to a more amorphous structure was further supported by the FTIR spectrum, exhibiting a broader O−H stretching peak.[22]

Morphological Characteristics of the CDAC Composite Film. The formulations containing MCC and carboxylated cellulose, both with and without HPMC, were found to be very brittle, breaking into small fragments due to the aggregation of MCC. This brittleness likely resulted from the high crystallinity of MCC and carboxylated cellulose, which hindered their dissolution or suspension in water. Consequently, they formed inhomogeneous mixtures that precipitated in the gelling solution, although carboxylated cellulose was easier to disperse and suspend than MCC. On the other hand, CDAC could be prepared as films due to its properties. CDAC not only possesses a more amorphous structure but also contains aldehyde groups that could enhance the water solubility. In hot water, the dialdehyde cellulose in the form of suspension provides a transparent solution that suspends without precipitation upon cooling to room temperature.[29] The addition of HPMC to CDAC further improved the overall water solubility, film appearance, and stability of the film matrix. CDAC and all CDAC composite films (D3H0, D2H1, D1.5H1.5, and D1H2) were homogeneous and slightly opaque without aggregation, while the HPMC film (D0H3) was homogeneous and translucent.

The thickness measurements of the films using a micrometer revealed that the D3H0 film had a thickness of 0.18 ± 0.01

https://doi.org/10.1021/acsomega.4c08298
ACS Omega 2024, 9, 44825−44836

Table 4. Mechanical Properties and Swelling Ratio of the CDAC Composite Films[a]

formulations	thickness (mm)	mechanical properties (mean ± S.D.)		swelling ratio (%)
		puncture strength (N/mm^2)	Young's modulus (N/mm^2)	
D3H0	0.18 ± 0.01	1.37 ± 0.21a	5.58 ± 1.18a	NA*
D2H1	0.09 ± 0.01	4.57 ± 0.75b	8.56 ± 1.27b	72.72 ± 6.35a
D1.5H1.5	0.10 ± 0.02	8.73 ± 1.73a	15.72 ± 3.88c	55.08 ± 5.42b
D1H2	0.11 ± 0.02	8.02 ± 0.89a	17.17 ± 1.99c	36.87 ± 4.92c
D0H3	0.09 ± 0.02	14.05 ± 2.92c	23.23 ± 3.77d	14.43 ± 4.49d

[a]Values in the same column with different lowercase letters (a−d) indicate significant differences between each formulation ($p < 0.05$). *NA (not applicable) means film disintegration.

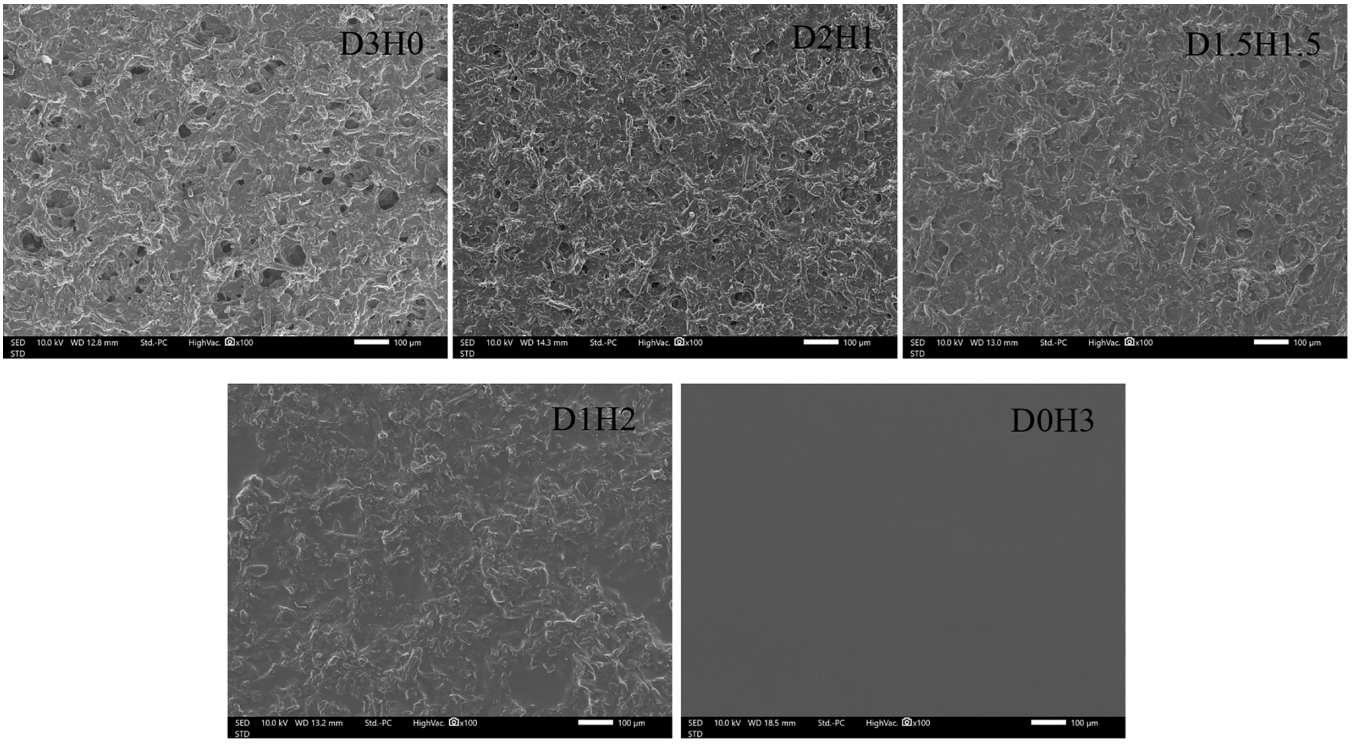

Figure 5. SEM micrographs showing surfaces of films.

mm. Upon the addition of HPMC, the thickness decreased, ranging from 0.08 to 0.12 mm in the following films: D2H1 (0.09 ± 0.01 mm), D1.5H1.5 (0.10 ± 0.02 mm), D1H2 (0.11 ± 0.02 mm), and D0H3 (0.09 ± 0.02 mm), as shown in Table 4. SEM micrographs of CDAC composite films are shown in Figures 5 and 6. The film surface of the CDAC composite films was homogeneous and rough, whereas the surface of D0H3 was smooth (Figure 5). Notably, the D3H0 film exhibited a large number of pores, and this number decreased as the CDAC ratio was reduced in the films (Figure 5). A similar trend was evident in the cross-sectional micrographs, where a higher number of pores were found in films with a higher ratio of CDAC (Figure 6). In contrast, the D0H3 film had a smooth matrix structure without visible pores. This study indicated that the addition of CDAC would increase the porosity of the CDAC composite films. A previous study reported that cellulose could increase the porosity of materials.[30] Another previous study reported that an increase in the cellulose ratio in PVA/cellulose aerogels has been shown to decrease density while increasing porosity.[29] The porosity of CDAC composite films has a significant effect on their mechanical and swelling properties.[31]

Mechanical Properties. The mechanical properties of the CDAC composite films are listed in Table 4. The puncture strength tended to increase as the CDAC ratio decreased. For example, the puncture strength of D3H0 was 1.37 ± 0.21 N/mm^2, while D1.5H1.5 and D2H1 exhibited 8.73 ± 1.73 and 4.57 ± 0.75 N/mm^2 of puncture strength, respectively. This suggests that the addition of CDAC to the formulations decreased the strength of CDAC composite films. Similarly, the Young's modulus decreased with increasing CDAC content. For instance, the Young's modulus of D0H3 was 23.23 ± 3.77 N/mm^2, while this value significantly dropped to 15.72 ± 3.88 and 8.56 ± 1.27 N/mm^2 in D1.5H1.5 and D2H1, respectively. These results can be attributed to the porosity of the films, as demonstrated by SEM micrographs. The more porous films are likely to have lower puncture strength and Young's modulus than the less porous films, indicating that the more porous films have less strength and stiffness, unlike the less porous films, which possess a loose film matrix.[32] The addition of copolymer could reduce the puncture strength of the HPMC film due to the nonuniform polymer chain.[33] The addition of CDAC not only introduced discontinuities in the film matrix and created pores, as observed in SEM micrographs, but also reduced intermolecular forces, thereby

https://doi.org/10.1021/acsomega.4c08298
ACS Omega 2024, 9, 44825−44836

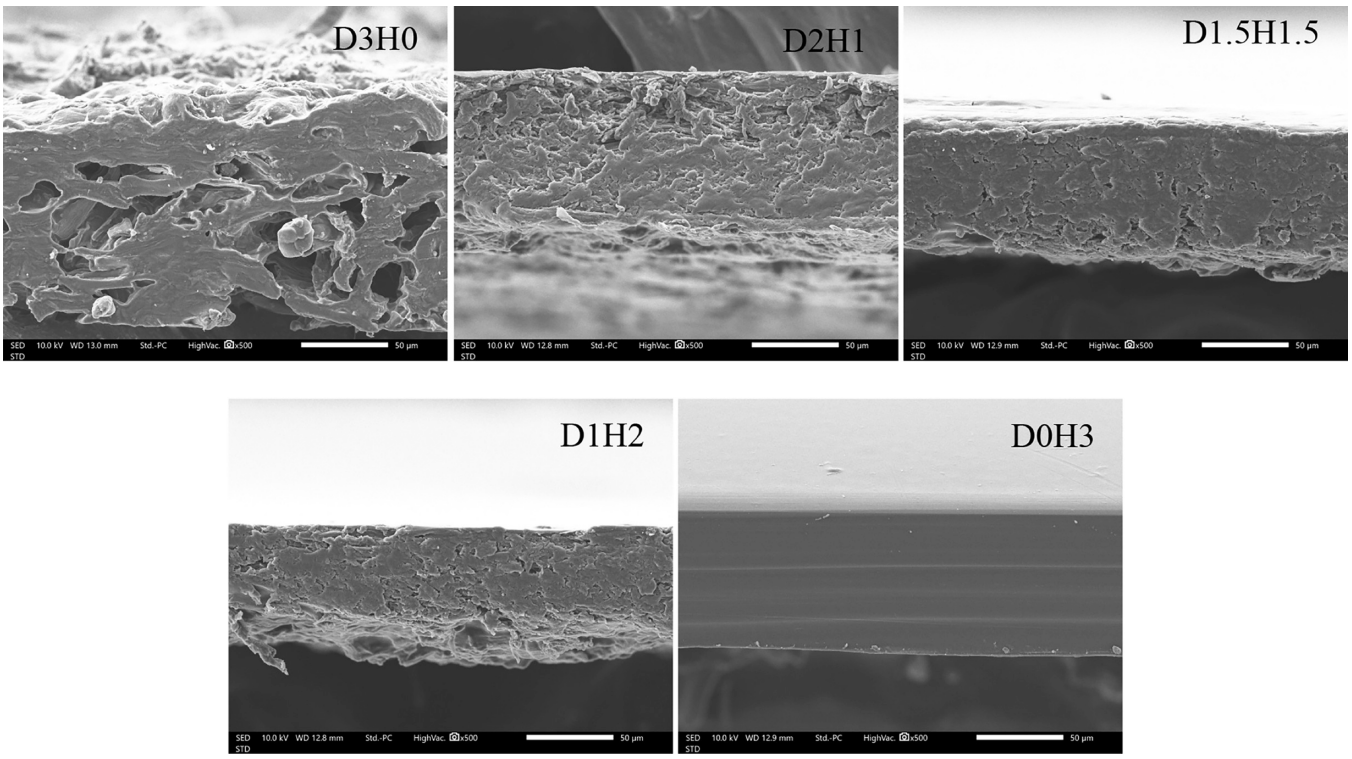

Figure 6. SEM micrographs showing the cross section of films.

increasing the mobility of the polymer chains. These factors contributed to decreases in the strength and stiffness of the composite films. Single-polymer films, such as pure HPMC films, typically provide a homogeneous matrix and a dense polymeric network. In contrast, pure CDAC films exhibited a porous matrix. When CDAC was added into the formulations, the polymer matrix became looser, resulting in reduced puncture strength and Young's modulus, particularly in the D2H1 formulation, which contained a higher amount of CDAC. A previous study found that the addition of another polymer in a composite film weakened the intramolecular interaction between polymers and decreased the packing density of the matrix.[1] Another previous study found that numerous holes and structural discontinuities were observed when chitosan was added to the sodium alginate film. It affected the mechanical properties of films.[34] D0H3 showed the highest puncture strength (14.05 ± 2.92 N/mm^2) and Young's modulus (23.23 ± 3.77 N/mm^2) since HPMC possesses good mechanical properties and a coherent structure. Furthermore, D0H3 displayed a dense film matrix. CDAC contains carboxylic and aldehyde groups, which can interact with the hydroxyl groups of HPMC via hydrophilic interactions, disrupting the polymeric network of HPMC. In this study, the film microstructure also influenced the mechanical properties. In other cases, such as chitosan/dialdehyde cellulose composite films, puncture strength and Young's modulus increased with higher ratios of dialdehyde cellulose due to cross-linking between the amide groups of chitosan and the aldehyde groups of dialdehyde cellulose.[35] Our study suggested that the addition of CDAC in a proper ratio could reduce puncture strength and Young's modulus of the CDAC/HPMC composite film, but the film composed of only CDAC exhibited poor mechanical properties.

Swelling Property. Unlike hydrogels, films are capable of absorbing certain types of fluid in a small volume. The swelling property refers to the water sorption capacity of each material. With good water sorption, wound dressing material would have various benefits, including improving wound exudate absorption, creating a moist environment for healing, promoting tissue regeneration, removing without tissue damage, and decreasing scar formation.[36,37] The swelling ratio of the CDAC composite films is shown in Table 4. The swelling ratio of D3H0 could not be measured since it disintegrated into small fragments without dissolution. That can be the result of, first, the numerous pores in the film matrix, which led to a loose structure. Second, the D3H0 film might lack an interaction between CDAC and HPMC, while the D0H3 film exhibited a low swelling ratio of 14.43 ± 4.49% due to the loss of film content. Basically, HPMC is soluble in water and gradually dissolves in film form. The D1H2 film exhibited a swelling ratio of 36.87 ± 4.92%, while the swelling ratios of the D1.5H1.5 and D2H1 films significantly increased to 55.08 ± 5.42 and 72.72 ± 6.35%, respectively. Generally, dialdehyde cellulose, including CDAC, does not dissolve in water at 32 °C. Therefore, the addition of CDAC could enhance the physical durability and delay the dissolution of HPMC. The D2H1 film shows the highest swelling ratio due to its higher porosity compared to the other films. An increase in void volume within a film matrix leads to greater water uptake, thereby increasing the swelling ratio.[38] In addition, CDAC contains both carboxylic and aldehyde groups, which are both hydrophilic and can interact with water molecules. Thus, the addition of CDAC increases the swelling property. A previous study found that water adsorption of aerogels increased with a higher content of dialdehyde cellulose in the formulations.[39]

https://doi.org/10.1021/acsomega.4c08298
ACS Omega 2024, 9, 44825−44836

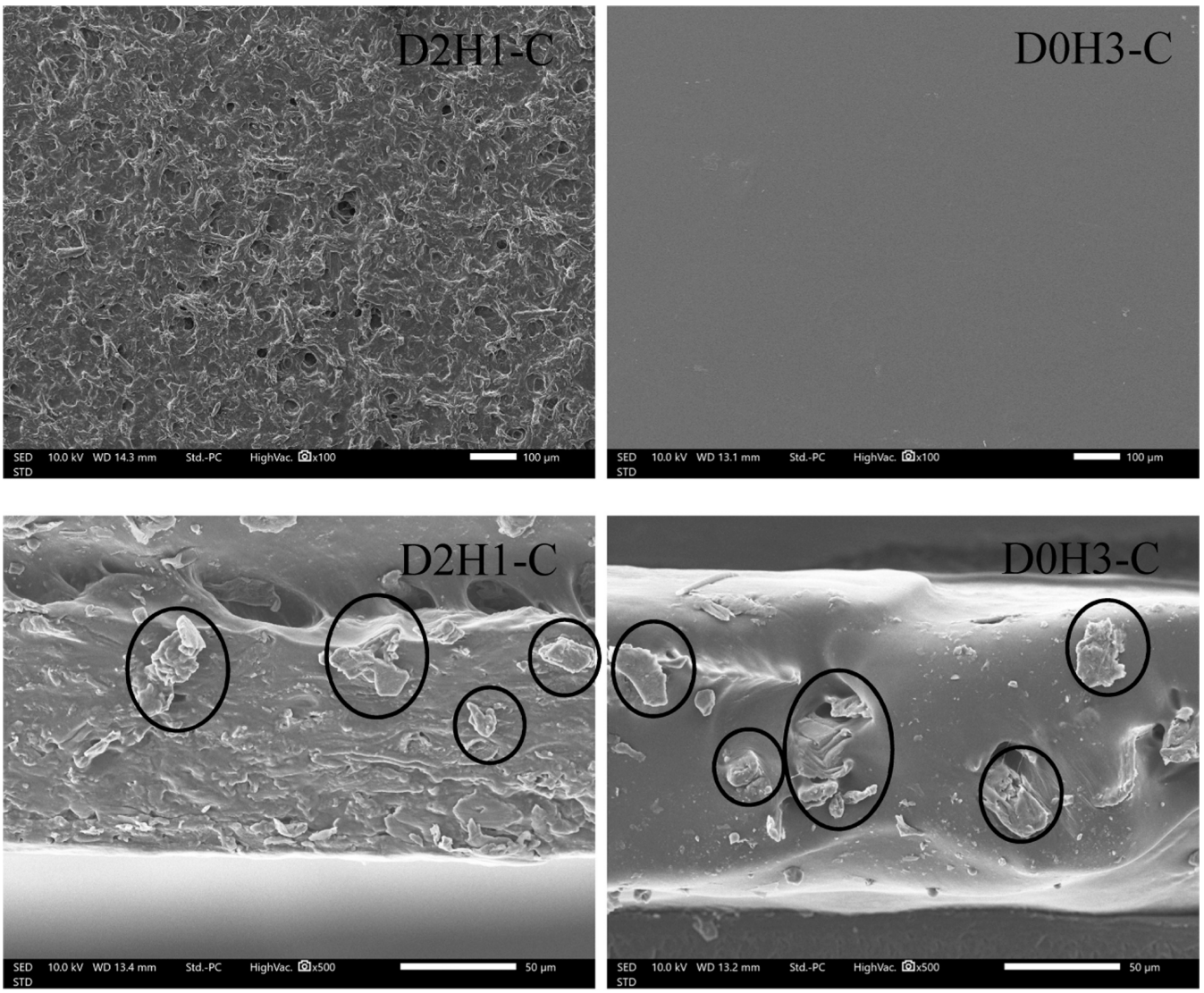

Figure 7. SEM micrographs showing the surface of D2H1-C and D0H3-C, and cross section of D2H1-C and D0H3-C.

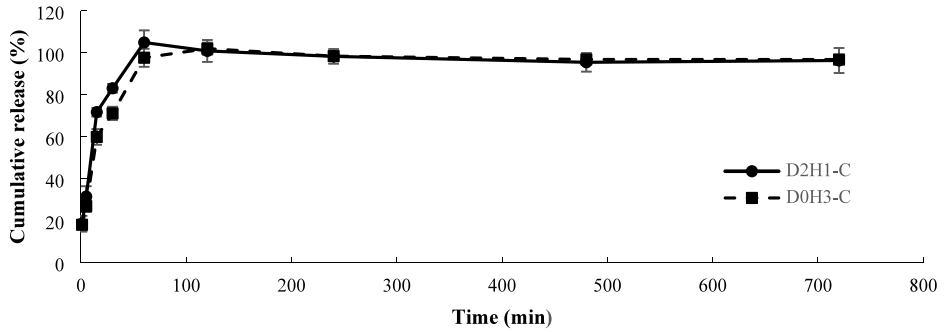

Figure 8. *In vitro* clindamycin release profile.

Morphological Characteristics of the CDAC Composite Film Loading Clindamycin HCl. The D2H1 formulation was selected to incorporate clindamycin HCl for antibacterial activity due to its suitable mechanical properties and swelling ratio. The SEM micrographs of D2H1 and D0H3 containing clindamycin HCl (D2H1-C and D0H3-C, respectively) are shown in Figure 7. D2H1-C exhibited a rough surface, similar to that of the D2H1 film (Figure 7). In contrast, D0H3-C displayed a smooth surface, consistent with the D0H3 film (Figure 7). Notably, the cross-sectional micrographs of D2H1-C and D0H3-C revealed the presence of clindamycin HCl crystals within the film matrix (Figure 7). This indicated that the clindamycin HCl was partially dissolved in the polymer matrix and that some parts remained in solid form due to recrystallization after drying.

Drug Loading Content. The drug content refers to the amount of drug loaded into the composite films. The D2H1-C and D0H3-C films exhibited high clindamycin HCl contents of

https://doi.org/10.1021/acsomega.4c08298
ACS Omega 2024, 9, 44825−44836

91.49 ± 5.48 and 92.72 ± 8.74%, respectively. These high drug contents can be attributed to two factors. First is the compatibility and complete dissolution of clindamycin HCl in the polymeric solution. Second is the high hydrophilicity of CDAC and HPMC that can react with clindamycin HCl. To clarify, CDAC contains carboxylic, aldehyde, and hydroxyl groups, while HPMC has a significant number of hydroxyl groups, both of which contribute to the high hydrophilicity.

***In Vitro* Drug Release Profile.** The clindamycin HCl release profile is shown in Figure 8. Both D2H1-C and D0H3-C exhibited immediate clindamycin HCl release. However, D2H1-C demonstrated a faster drug release than D0H3-C and over 80% of the drug was released within 30 min. Initially, there was no significant difference in cumulative release between the two films. At 15 min, the cumulative release of D2H1-C was 71.77 ± 2.08% and reached 83.14 ± 1.82% at 30 min, while D0H3-C exhibited significantly lower cumulative release (59.95 ± 3.70 and 71.19 ± 3.17% at 15 and 30 min, respectively) compared to D2H1-C. The rapid release of clindamycin HCl is attributed not only to the drug's water solubility but also to the properties of the films. The hydrophilic nature and high swelling ratio of the films facilitated rapid drug release.[40] The primary mechanism of drug release from hydrophilic polymers involves polymer swelling.[41] When polymer swells, a drug dissolves or diffuses toward the outside of the matrix due to the entry of water into the matrix.[42] In addition, a previous study reported that the hydrogel film with low mechanical strength released drug rapidly.[40] Thus, the D2H1 film, with its higher swelling ratio and lower mechanical strength, exhibited faster clindamycin HCl release.

Antibacterial Test. The antibacterial activity of the CDAC composite films is shown in Table 5. The clindamycin disk used as the positive control showed antibacterial activity against *S. aureus* (MSSA) and *S. aureus* (MRSA) because, basically, clindamycin has good antibacterial activity against *S. aureus* but is not effective against *P. aeruginosa*. D0H3 did not exhibit antibacterial activity against any bacterial strains, as it lacks inherent antibacterial properties. The D0H3-C film was effective against both strains of *S. aureus* due to the antibacterial activity of clindamycin. Interestingly, the D2H1 film showed antibacterial activity against *S. aureus* (MSSA), *S. aureus* (MRSA), and *P. aeruginosa*. Previous studies reported that dialdehyde groups provided antibacterial activity against *S. aureus* and *P. aeruginosa*.[1,43] The antibacterial activity of the D2H1 film was attributed to dialdehyde groups, and it correlated with aldehyde content of modified celluloses, which should be more than 60%.[1,10,44] There were a few mechanisms of antibacterial activity. A previous study suggested that dialdehyde MCC cross-links with bacterial proteins and nucleic acids through a Schiff base reaction, leading to microbial inactivation.[45] This mechanism is similar to that of glutaraldehyde, while dialdehyde groups of cellulose have the advantage of nontoxicity.[46] The D2H1-C film was effective in inhibiting all tested bacteria, and its antibacterial activity increased significantly ($p < 0.05$) compared to the D2H1 film due to the synergistic effect between clindamycin HCl and CDAC. In addition, this study found that CDAC could enhance antibacterial activity of clindamycin HCl to be effective against *P. aeruginosa*. Therefore, CDAC had a great promise as a composite material for enhancing antibacterial activity.

Table 5. Antibacterial Activity of CDAC Composite Films[a]

samples	zone of inhibition (mm)		
	S. aureus (MSSA)	*S. aureus* (MRSA)	*P. aeruginosa*
clindamycin disk (2 μg)	23.0 ± 0.0a	24.0 ± 0.6a	0a
D0H3 film	0b	0b	0a
D0H3-C film	34.67 ± 0.58c	27 ± 0.6c	0a
D2H1 film	10.0 ± 2.0d	20.7 ± 1.2d	10.7 ± 1.2b
D2H1-C film	35.0 ± 1.0c	35.3 ± 0.58e	22.7 ± 0.6c

[a]Values in same column with different lowercase letters (a−e) indicate significant differences between each sample ($p < 0.05$).

CONCLUSIONS

CDAC was synthesized from MCC through oxidation using $FeSO_4 \cdot 7H_2O$ and $NaIO_4$ to obtain carboxylic and dialdehyde groups, respectively. The obtained CDAC contained 2.1 ± 0.2 carboxylate content and 4.15 ± 0.2 mmol/g of aldehyde content (equivalent to 67.23 ± 3.24%). FTIR spectra showed characteristic peaks of carboxylic and dialdehyde groups. Due to the synthesis process, CDAC exhibited greater amorphousness compared to carboxylated cellulose and MCC. The study revealed that the ratio of CDAC to HPMC influenced the properties of the composite films. The porosity of the composite films increased with a higher ratio of CDAC due to the disruption of the film matrix by CDAC. The puncture strength and Young's modulus decreased when the ratio of CDAC in the films increased. The D2H1 film exhibited a higher swelling ratio than others. The D2H1 film was deemed the most suitable for loading clindamycin HCl as an antibacterial agent due to its superior appearance, mechanical strength, and swelling properties compared to other formulations. Both D2H1 and D0H3 films exhibited high drug content (91.49 ± 5.48 and 92.72 ± 8.74%, respectively) and immediate drug release. D2H1 released clindamycin more rapidly than D0H3, which was attributed to its higher swelling ratio and lower mechanical strength. Interestingly, the D2H1 film was effective against *S. aureus* (MSSA), *S. aureus* (MRSA) and *P. aeruginosa*, because of the antibacterial activity of CDAC from dialdehyde groups. Furthermore, CDAC enhanced the antibacterial activity of clindamycin HCl against *S. aureus* (MSSA) and *S. aureus* and provided the ability to inhibit growth of *P. aeruginosa*. These results were found in the D2H1-C film. This study highlights the potential of CDAC as a key component in antibacterial materials for wound dressing applications. However, further studies, including toxicity assessments, are necessary to confirm the safety for clinical use.

AUTHOR INFORMATION

Corresponding Author

Tanpong Chaiwarit − *Department of Pharmaceutical Sciences, Faculty of Pharmacy, Chiang Mai University, Chiang Mai 50200, Thailand;* orcid.org/0009-0009-5531-4692; Email: Tanpong.ch@cmu.ac.th

Authors

Kwanjit Duangsonk − *Department of Microbiology, Faculty of Medicine, Chiang Mai University, Chiang Mai 50200, Thailand*

https://doi.org/10.1021/acsomega.4c08298
ACS Omega 2024, 9, 44825−44836

Sastra Yuantrakul − *Department of Microbiology, Faculty of Medicine, Chiang Mai University, Chiang Mai 50200, Thailand*

Baramee Chanabodeechalermrung − *Department of Pharmaceutical Sciences, Faculty of Pharmacy, Chiang Mai University, Chiang Mai 50200, Thailand*

Waristha Khangtragool − *Department of Pharmaceutical Sciences, Faculty of Pharmacy, Chiang Mai University, Chiang Mai 50200, Thailand*

Claire-Hélène Brachais − *ICMUB UMR CNRS 6302, University of Bourgogne Franche-Comté, Dijon 21000, France*

Odile Chambin − *Department of Pharmaceutical Technology, UMR PAM, University of Bourgogne, Dijon 21079, France;* orcid.org/0000-0002-9627-6073

Pensak Jantrawut − *Department of Pharmaceutical Sciences, Faculty of Pharmacy, Chiang Mai University, Chiang Mai 50200, Thailand; Center of Excellence in Agro Bio-Circular-Green Industry (Agro BCG), Chiang Mai University, Chiang Mai 50100, Thailand*

Complete contact information is available at: https://pubs.acs.org/10.1021/acsomega.4c08298

Author Contributions

T.C., investigation, writing—original draft, methodology, supervision, and writing—review and editing; K.D., investigation and methodology; S.Y., investigation and methodology; B.C., investigation and methodology; W.K., investigation and methodology; C.-H.B., investigation, methodology, and validation; O.C., investigation, methodology, and validation; P.J., investigation, methodology, writing—original draft, methodology, and writing—review and editing. The manuscript was written through contributions of all authors. All authors have given approval to the final version of the manuscript.

Notes

The authors declare no competing financial interest.

■ ACKNOWLEDGMENTS

This research has received funding support from the NSRF via the Program Management Unit for Human Resources & Institutional Development, Research and Innovation [grant number B13F660085]. This research has been supported by the CMU Junior Research Fellowship Program and Franco-Thai Young Talent Research Fellowship Program 2023.

■ ABBREVIATIONS

CDAC, carboxylate-dialdehyde cellulose; MCC, microcrystalline cellulose; HPMC, hydroxypropyl methylcellulose; FTIR, Fourier transform infrared; XRD, X-ray diffractometry; SEM, scanning electron microscopy; PBS, phosphate-buffered saline

■ REFERENCES

(1) Mayer, S.; Tallawi, M.; De Luca, I.; Calarco, A.; Reinhardt, N.; Gray, L. A.; Drechsler, K.; Moeini, A.; Germann, N. Antimicrobial and physicochemical characterization of 2,3-dialdehyde cellulose-based wound dressings systems. *Carbohydr. Polym.* **2021**, *272*, 118506.

(2) Liu, Y.; Bai, L.; Zhu, X.; Xu, D.; Li, G.; Liang, H.; Wiesner, M. R. The role of carboxylated cellulose nanocrystals placement in the performance of thin-film composite (TFC) membrane. *J. Membr. Sci.* **2021**, *617*, 118581.

(3) Shi, C.; Wang, C.; Liu, H.; Li, Q.; Li, R.; Zhang, Y.; Liu, Y.; Shao, Y.; Wang, J. Selection of Appropriate Wound Dressing for Various Wounds. *Front. Bioeng. Biotechnol.* **2020**, *8*, 182.

(4) Savencu, I.; Iurian, S.; Porfire, A.; Bogdan, C.; Tomuţă, I. Review of advances in polymeric wound dressing films. *React. Funct. Polym.* **2021**, *168*, 105059.

(5) Rezvanian, M.; Amin, M. C. I. M.; Ng, S.-F. Development and physicochemical characterization of alginate composite film loaded with simvastatin as a potential wound dressing. *Carbohydr. Polym.* **2016**, *137*, 295−304.

(6) Kujath, P.; Michelsen, A. Wounds - from physiology to wound dressing. *Dtsch. Ärzteblatt Int.* **2008**, *105* (13), 239−248.

(7) Zeng, J.; Xiong, X.; Hu, F.; Li, J.; Li, P. dialdehyde Cellulose Solution as Reducing Agent: Preparation of Uniform Silver Nanoparticles and In Situ Synthesis of Antibacterial Composite Films with High Barrier Properties. *Molecules* **2023**, *28* (7), 2956.

(8) Madivoli, E. S.; Kareru, P. G.; Gachanja, A. N.; Mugo, S. M.; Makhanu, D. S. Synthesis and characterization of dialdehyde cellulose nanofibers from O. sativa husks. *SN Appl. Sci.* **2019**, *1* (7), 723.

(9) Fan, X.-M.; Yu, H.-Y.; Wang, D.-C.; Mao, Z.-H.; Yao, J.; Tam, K. C. Facile and Green Synthesis of Carboxylated Cellulose Nanocrystals as Efficient Adsorbents in Wastewater Treatments. *ACS Sustainable Chem. Eng.* **2019**, *7* (21), 18067−18075.

(10) Ge, H.; Zhang, L.; Xu, M.; Cao, J.; Kang, C. Preparation of dialdehyde Cellulose and Its Antibacterial Activity, In *Advances in Applied Biotechnology*, Liu, H.; Song, C.; Ram, A., Eds. Singapore: Springer Singapore, 2018; pp 545−553.

(11) Chen, L.; Dong, Q.; Shi, Q.; Du, Y.; Zeng, Q.; Zhao, Y.; Wang, J. J. Novel 2,3-dialdehyde Cellulose-Based Films with Photodynamic Inactivation Potency by Incorporating the β-Cyclodextrin/Curcumin Inclusion Complex. *Biomacromolecules* **2021**, *22* (7), 2790−2801.

(12) Luchian, I.; Goriuc, A.; Martu, M. A.; Covasa, M. Clindamycin as an Alternative Option in Optimizing Periodontal Therapy. *Antibiotics* **2021**, *10* (7), 814.

(13) Hasan, N.; Cao, J.; Lee, J.; Kim, H.; Yoo, J.-W. Development of clindamycin-loaded alginate/pectin/hyaluronic acid composite hydrogel film for the treatment of MRSA-infected wounds. *Journal of Pharmaceutical Investigation* **2021**, *51* (5), 597−610.

(14) Sadeghi, S.; Nourmohammadi, J.; Ghaee, A.; Soleimani, N. Carboxymethyl cellulose-human hair keratin hydrogel with controlled clindamycin release as antibacterial wound dressing. *Int. J. Biol. Macromol.* **2020**, *147*, 1239−1247.

(15) Zhao, H.; Zhang, K.; Rui, S.; Zhao, P. Study on microcrystalline cellulose/chitosan blend foam gel material. *Science and Engineering of Composite Materials* **2020**, *27* (1), 424−432.

(16) Wang, X.; Le, H.; Guo, Y.; Zhao, Y.; Deng, X.; Zhang, J.; Zhang, L. Preparation of Cellulose Nanocrystals from Jujube Cores by Fractional Purification. *Molecules* **2022**, *27* (10), 3236.

(17) Chaiwarit, T.; Rachtanapun, P.; Kantrong, N.; Jantrawut, P. Preparation of Clindamycin Hydrochloride Loaded De-Esterified Low-Methoxyl Mango Peel Pectin Film Used as a Topical Drug Delivery System. *Polymers* **2020**, *12* (5), 1006.

(18) Otoni, C. G.; Moura, M. R. d.; Aouada, F. A.; Camilloto, G. P.; Cruz, R. S.; Lorevice, M. V.; Soares, N. d. F. F.; Mattoso, L. H. C. Antimicrobial and physical-mechanical properties of pectin/papaya puree/cinnamaldehyde nanoemulsion edible composite films. *Food hydrocolloids* **2014**, *41*, 188−194.

(19) Lousada, C. M.; Yang, M.; Nilsson, K.; Jonsson, M. Catalytic decomposition of hydrogen peroxide on transition metal and lanthanide oxides. *J. Mol. Catal. A: Chem.* **2013**, *379*, 178−184.

(20) Kargarzadeh, H.; Ahmad, I.; Abdullah, I.; Dufresne, A.; Zainudin, S. Y.; Sheltami, R. M. Effects of hydrolysis conditions on the morphology, crystallinity, and thermal stability of cellulose nanocrystals extracted from kenaf bast fibers. *Cellulose* **2012**, *19* (3), 855−866.

(21) Varma, A. J.; Kulkarni, M. P. Oxidation of cellulose under controlled conditions. *Polym. Degrad. Stab.* **2002**, *77* (1), 25−27.

(22) Plappert, S. F.; Quraishi, S.; Pircher, N.; Mikkonen, K. S.; Veigel, S.; Klinger, K. M.; Potthast, A.; Rosenau, T.; Liebner, F. W.

Transparent, Flexible, and Strong 2,3-dialdehyde Cellulose Films with High Oxygen Barrier Properties. *Biomacromolecules* **2018**, *19* (7), 2969−2978.
(23) Yang, H.; Chen, D.; van de Ven, T. G. M. Preparation and characterization of sterically stabilized nanocrystalline cellulose obtained by periodate oxidation of cellulose fibers. *Cellulose* **2015**, *22* (3), 1743−1752.
(24) Liang, H.; Liu, K.; Ni, Y. Synthesis of mesoporous α-Fe2O3 using cellulose nanocrystals as template and its use for the removal of phosphate from wastewater. *Journal of the Taiwan Institute of Chemical Engineers* **2017**, *71*, 474−479.
(25) Fan, Q. G.; Lewis, D. M.; Tapley, K. N. Characterization of cellulose aldehyde using Fourier transform infrared spectroscopy. *J. Appl. Polym. Sci.* **2001**, *82* (5), 1195−1202.
(26) Kian, L. K.; Jawaid, M.; Ariffin, H.; Alothman, O. Y. Isolation and characterization of microcrystalline cellulose from roselle fibers. *Int. J. Biol. Macromol.* **2017**, *103*, 931−940.
(27) Cheng, M.; Qin, Z.; Liu, Y.; Qin, Y.; Li, T.; Chen, L.; Zhu, M. Efficient extraction of carboxylated spherical cellulose nanocrystals with narrow distribution through hydrolysis of lyocell fibers by using ammonium persulfate as an oxidant. *Journal of Materials Chemistry A* **2014**, *2* (1), 251−258.
(28) Leguy, J.; Diallo, A.; Putaux, J.-L.; Nishiyama, Y.; Heux, L.; Jean, B. periodate Oxidation Followed by NaBH4 Reduction Converts Microfibrillated Cellulose into Sterically Stabilized Neutral Cellulose Nanocrystal Suspensions. *Langmuir* **2018**, *34* (37), 11066−11075.
(29) Kim, U.-J.; Wada, M.; Kuga, S. Solubilization of dialdehyde cellulose by hot water. *Carbohydr. Polym.* **2004**, *56* (1), 7−10.
(30) Nguyen, T. T. V.; Tri, N.; Tran, B. A.; Dao Duy, T.; Nguyen, S. T.; Nguyen, T.-A.; Phan, A. N.; Mai Thanh, P.; Huynh, H. K. P. Synthesis, Characteristics, Oil Adsorption, and Thermal Insulation Performance of Cellulosic Aerogel Derived from Water Hyacinth. *ACS Omega* **2021**, *6* (40), 26130−26139.
(31) van Bochove, B.; Grijpma, D. W. Mechanical properties of porous photo-crosslinked poly(trimethylene carbonate) network films. *Eur. Polym. J.* **2021**, *143*, 110223.
(32) Ghadermazi, R.; Hamdipour, S.; Sadeghi, K.; Ghadermazi, R.; Khosrowshahi Asl, A. Effect of various additives on the properties of the films and coatings derived from hydroxypropyl methylcellulose—A review. *Food Sci. Nutr.* **2019**, *7* (11), 3363−3377.
(33) Wang, Y.; Jiang, S.; Chen, Y.; Qiu, D.; Weng, Y. Synthesis and Characterization of a Novel Composite Edible Film Based on Hydroxypropyl Methyl Cellulose Grafted with Gelatin. *Gels* **2023**, *9* (4), 332.
(34) Gao, C.; Wang, S.; Liu, B.; Yao, S.; Dai, Y.; Zhou, L.; Qin, C.; Fatehi, P. Sustainable Chitosan-dialdehyde Cellulose Nanocrystal Film. *Materials* **2021**, *14* (19), 5851.
(35) He, M.; Zheng, Y.; Shen, J.; Shi, J.; Zhang, Y.; Xiao, Y.; Che, J. Chitosan/Sodium Alginate Multilayer pH-Sensitive Films Based on Layer-by-Layer Self-Assembly for Intelligent Packaging. *J. Renewable Mater.* **2024**, *12* (2), 215−233.
(36) Dong, F.; Li, S. Wound Dressings Based on Chitosan-dialdehyde Cellulose Nanocrystals-Silver Nanoparticles: Mechanical Strength, Antibacterial Activity and Cytotoxicity. *Polymers* **2018**, *10* (6), 673.
(37) Chen, H.; Lan, G.; Ran, L.; Xiao, Y.; Yu, K.; Lu, B.; Dai, F.; Wu, D.; Lu, F. A novel wound dressing based on a Konjac glucomannan/silver nanoparticle composite sponge effectively kills bacteria and accelerates wound healing. *Carbohydr. Polym.* **2018**, *183*, 70−80.
(38) Gupta, N. V.; Shivakumar, H. G. Investigation of Swelling Behavior and Mechanical Properties of a pH-Sensitive Superporous Hydrogel Composite. *Iran. J. Pharm. Res.* **2012**, *11* (2), 481−493.
(39) Lu, T.; Li, Q.; Chen, W.; Yu, H. Composite aerogels based on dialdehyde nanocellulose and collagen for potential applications as wound dressing and tissue engineering scaffold. *Compos. Sci. Technol.* **2014**, *94*, 132−138.
(40) Ghauri, Z. H.; Islam, A.; Qadir, M. A.; Gull, N.; Haider, B.; Khan, R. U.; Riaz, T. Development and evaluation of pH-sensitive biodegradable ternary blended hydrogel films (chitosan/guar gum/PVP) for drug delivery application. *Sci. Rep.* **2021**, *11* (1), 21255.
(41) Kevadiya, B. D.; Zhang, L.; Davé, R. N. Sustained Release of Poorly Water-Soluble Drug from Hydrophilic Polymeric Film Sandwiched Between Hydrophobic Layers. *AAPS PharmSciTech* **2018**, *19* (6), 2572−2584.
(42) Maderuelo, C.; Zarzuelo, A.; Lanao, J. M. Critical factors in the release of drugs from sustained release hydrophilic matrices. *J. Controlled Release* **2011**, *154* (1), 2−19.
(43) Hasanin, M.; Hashem, A. H.; El-Rashedy, A. A.; Kamel, S. Synthesis of novel heterocyclic compounds based on dialdehyde cellulose: characterization, antimicrobial, antitumor activity, molecular dynamics simulation and target identification. *Cellulose* **2021**, *28* (13), 8355−8374.
(44) Kokol, V.; Novak, S.; Kononenko, V.; Kos, M.; Vivod, V.; Gunde-Cimerman, N.; Drobne, D. Antibacterial and degradation properties of dialdehyded and aminohexamethylated nanocelluloses. *Carbohydr. Polym.* **2023**, *311*, 120603.
(45) Zhang, L.; Ge, H.; Xu, M.; Cao, J.; Dai, Y. Physicochemical properties, antioxidant and antibacterial activities of dialdehyde microcrystalline cellulose. *Cellulose* **2017**, *24* (5), 2287−2298.
(46) Muchová, M.; Münster, L.; Capáková, Z.; Mikulcová, V.; Kuřitka, I.; Vícha, J. Design of dialdehyde cellulose crosslinked poly(vinyl alcohol) hydrogels for transdermal drug delivery and wound dressings. *Materials Science and Engineering: C* **2020**, *116*, 111242.

https://doi.org/10.1021/acsomega.4c08298
ACS Omega 2024, 9, 44825−44836